

STIP1 Regulates Proliferation and Migration of Lung Adenocarcinoma Through JAK2/STAT3 Signaling Pathway

This article was published in the following Dove Press journal:
Cancer Management and Research

Xiangjun Guo^{1,2}
Zhongyi Yan²
Gongming Zhang²
Xiang Wang²
Yun Pan²
Mao Huang¹

¹Department of Respiratory and Critical Care Medicine, The First Affiliated Hospital of Nanjing Medical University, Nanjing, People's Republic of China;

²Department of Respiratory and Critical Care Medicine, The First People's Hospital of Lianyungang, Lianyungang, Jiang su, People's Republic of China

Purpose: Recent studies have shown that STIP1 is associated with proliferation and migration in numerous types of tumors; however, the role of STIP1 in lung adenocarcinoma is still poorly understood. Therefore, the aim of this study was to evaluate the role of STIP1 in lung adenocarcinoma, in vitro and in vivo.

Methods: The expression of STIP1 in lung adenocarcinoma was assessed by immunohistochemistry, RT-qPCR, and Western blot. The effects of STIP1 on the proliferation of lung adenocarcinoma cells were detected by the cell counting kit-8 assay; the effect of STIP1 on adhesion of lung adenocarcinoma cells was detected by Giemsa staining, while the cell scratch and Transwell assays were employed to examine the effect of STIP1 on the migratory ability of lung adenocarcinoma cells. Finally, apoptosis was evaluated by Hoechst staining and flow cytometry.

Results: The expression level of STIP1 in lung adenocarcinoma tissue was significantly higher than that in adjacent normal tissue ($P < 0.05$). Compared with that in nontransfected controls, cell proliferation, adhesion, and migration, as well as vimentin protein expression and levels of phosphorylated JAK2/STAT3, were significantly decreased ($P < 0.05$) in A549 lung adenocarcinoma cells transfected with STIP1 shRNA, whereas E-cadherin protein expression and rates of apoptosis were significantly increased in these cells ($P < 0.05$).

Conclusion: Elevated expression of STIP1 in lung adenocarcinoma may enhance the proliferative, adhesive, and migratory ability, and reduce the apoptosis of lung adenocarcinoma cells through the JAK2/STAT3 signaling pathway and epithelial-mesenchymal transition (EMT), thereby promoting the recurrence and metastatic potential of this cancer. The results indicate that STIP1 may be an effective therapeutic target for the treatment of lung adenocarcinoma.

Keywords: STIP1, JAK2/STAT3, lung adenocarcinoma

Introduction

According to the 2018 Global Cancer Statistics report published online in the Journal of clinicians Cancer¹ and the latest issue of national cancer statistics released by the China Cancer Center,² lung cancer is the leading cause of death and the most commonly occurring cancer worldwide. Non-small cell lung cancer (NSCLC) is the main pathological classification among the different types of lung cancer. Although several treatment methods for NSCLC are currently available, including surgery, radiotherapy, chemotherapy, targeted therapy, and immunotherapy, 75% of lung cancer patients are diagnosed at a late stage, and the 5-year

Correspondence: Mao Huang
Department of Respiratory and Critical Care Medicine, The First Affiliated Hospital of Nanjing Medical University, Nanjing, People's Republic of China
Tel +86 1381388616
Email huangmao6116@126.com

survival rate is low. Consequently, it is critical that the pathogenesis, recurrence, and metastatic potential of NSCLC are exhaustively characterized and effective therapeutic targets identified.

At present, tumor cell metastasis is the primary reason for the poor efficacy of NSCLC treatment. Epithelial–mesenchymal transition (EMT) is crucial for tumor metastasis, and involves the activity of various regulatory factors that promote the downregulation of E-cadherin expression and upregulation of the expression of interstitial cell markers, such as N-cadherin, on cancer cell membranes. Furthermore, EMT leads to loss of adhesion, as well as changes in the polarity and morphology of cancer cells, both of which are involved in tumor invasion and metastasis.^{3,4} Several studies have found that the regulatory factors and signaling pathways associated with EMT are complex and variable. The JAK2/STAT3 signaling pathway is known to regulate epithelial cell–cell adhesion and is closely related to the occurrence of EMT in malignant lesions.^{5–7} In colorectal cancer, this pathway influences tumor cell activity by regulating the expression of BCL2, E-cadherin, and VEGF, among others,⁸ while in ovarian cancer, activated STAT3 can promote the occurrence of EMT through the JAK2/STAT3/Snail signaling pathway.⁹ Furthermore, albumin can induce cell proliferation and transdifferentiation of renal tubular epithelial cells by activating the JAK2/STAT3 signaling pathway.¹⁰ However, reports on the correlation between JAK2/STAT3 signaling and EMT in lung adenocarcinoma are limited.

Stress-induced phosphoprotein1 (STIP1), also known as HOP (HSP70/HSP90-organizing protein), is a protein with a molecular weight of 62.6 kDa that was first identified in *Saccharomyces cerevisiae*.¹¹ STIP1 contains three tetratricopeptide repeat (TPR) domains, which provide the structural basis for its function.¹² STIP1 interacts with members of the heat-shock protein family through these domains and mediates the association between HSP70 and HSP90, forming a multiprotein complex by hydrolyzing the mutual transformation between ATP and ADP, which is involved in the splicing and transcription of RNA and the folding of proteins.^{13,14} Several studies have shown that STIP1 is overexpressed in, and contributes to, the development of a variety of human malignant tumors, including hepatocellular carcinoma,¹⁵ glioblastoma,¹⁶ pancreatic cancer,¹⁷ colon cancer,¹⁸ cervical cancer,¹⁹ and thyroid papilla carcinoma with lymph node metastasis.²⁰ These observations suggest that STIP1 may play a crucial role in tumor occurrence and progression.

Although numerous studies have evaluated the role of STIP1 in tumors, reports on the roles of STIP1 in lung adenocarcinoma are limited. The results of this study showed that elevated levels of STIP1 induce lung adenocarcinoma cell proliferation and migration through the JAK2/STAT3 signaling pathway and regulation of EMT. Reducing the expression of STIP1 in lung adenocarcinoma may help to suppress EMT processes in lung adenocarcinoma cells and decrease tumor proliferation and migration, indicating that STIP1 has potential as a therapeutic target for the treatment of lung adenocarcinoma, and practical clinical significance.

Materials and Methods

Patients

Forty-eight lung adenocarcinoma and Thirty-two lung squamous cell carcinoma tissue samples, as well as corresponding paracancerous tissue, were collected from the Department of Pathology of the First People's Hospital of Lianyungang City from January 2015 to February 2019. The patients and their families agreed to participate in the study and signed an informed consent form. The study was approved by the Ethics Committee of the First People's Hospital of Lianyungang City. Fresh pathological tissue was immediately frozen in liquid nitrogen for 30 min, and then stored at -80°C until used for PCR and Western blot analyses. STIP1 protein expression in lung adenocarcinoma and squamous cell carcinoma was assessed by hematoxylin and eosin (H&E) and immunohistochemical staining.

Cell Culture

Our all cell lines were purchased from the Shanghai Institutes for Biological Sciences, Chinese Academy of Sciences. The cells were reheated in warm water at 40°C , suspended in 10 mL of medium supplemented with 10% fetal bovine serum (FBS), and then centrifugated at $1500 \times g$ for 5 min. After centrifugation, the supernatants were discarded and the cells resuspended. The cells were subsequently inoculated in 6-cm dishes and cultured in an incubator at 37°C with 5% CO_2 . The growth status of the cells was observed daily.

Animals

Eighteen male BALB/c nude mice (aged 6–8 weeks) were obtained from Sbeifu Biotechnology Co., Ltd. The mice were fed and raised separately under specific-pathogen-free (SPF) conditions in the laboratory. The mice were maintained under

appropriate temperature and humidity conditions, and body weight was measured every other day. The animal use protocol has been reviewed and approved by the Animal Ethical and Welfare Committee (AEWC) of Nanjing Medical University.

Immunohistochemistry

All paraffin-embedded sections were stained using a Ventana automatic immunohistochemical apparatus (Roche, Switzerland). The rabbit anti-human STIP1 monoclonal antibody (ab126724, 1:500) was purchased from Abcam (USA). The positive controls were mouse myocardial and human serous ovarian cancer sections, and PBS instead of primary antibody was used as the negative control. The immunohistochemistry score was independently validated by two pathologists. The cell staining intensity was classified into 4 levels (0–3+) (0, no staining; 1, low staining; 2, moderate staining; 3, strong staining), while the percentage of stained cells was classified into 4 grades (0, <10%; 1, 10–24%; 2, 25–50%; 3, >50%). The two values were multiplied to obtain the immunohistochemical (IHC) score and evaluate the intensity of immunohistochemical staining.²¹ All the IHC scores were repeated three times using a double-blind method.

Western Blot

Samples containing equal protein concentrations were added to 4× protein loading buffer and boiled in a water bath for 5 min. Proteins were separated by sodium dodecyl sulfate–polyacrylamide gel electrophoresis (SDS–PAGE) and then transferred to wet PVDF membranes. The modified membranes were sealed in 5% milk for 3 h, and then incubated with the respective primary antibodies (anti-STIP1 [1:2000], anti-JAK2 [1:1000], anti-beta-actin [1:5000], Proteintech; anti-pJAK2 [1:1000], Affinity; anti-STAT3 and anti-p-STAT3 [1:1000], Cell Signaling) at 4 °C overnight. After washing, the membranes were incubated with horseradish peroxidase (HRP)-labeled secondary antibodies at room temperature for 50 min. Beta-actin was used as the internal control.

Real-Time Quantitative PCR

Total RNA was isolated using the Total-RNA isolation kit (Invitrogen). Real-time quantitative PCR (RT-qPCR) was performed using SYBR Green (TaKaRa) according to the manufacturer's instructions. The amplification conditions were as follows: preincubation at 95°C for 15 min, followed by 40 cycles of 95°C for 10 s and 60 °C for 30 s. mRNA

was quantified using the $2^{-\Delta\Delta Ct}$ method and *GAPDH* served as the internal control. The sequences of the *STIP1*-specific primers used in this study were as follows: *STIP1* forward 5'-GCCAAGCGAACCTATGAGGAG-3'; reverse 5'-GGATCACTGAGTAGTGTCTTGT-3'.

STIP1 shRNA Design and Synthesis

The *STIP1* gene sequence was obtained from GenBank. The designed oligonucleotide sequences were cloned into the pGPU6 vector. The *STIP1* short hairpin RNA (shRNA) and non-specific shRNA (negative control, NC) used in this study were as follows: *STIP1* shRNA chain: 5'-CACCGCTAAACATCTGAATTGGCTCTTCAAGAGAGAGAGCCAATT-CAGATGGTTTAGTTTTTTG-3'; *STIP1* shRNA NC chain: 5'-CACCGTTCTCCGAACGTGTCACGTCAAGAGATTACGTGACACGTTCCGAGAATTTTTTTG-3'.

Cell Transfection

Transfection of shRNA was carried out using lipofectamine 2000 (Invitrogen) following the manufacturer's instructions. Briefly, cells were seeded at a concentration of 2×10^5 cells/dish (6cm) and grown to 70% confluence. Lipofectamine 2000 and shRNA were then mixed and the mixture was incubated in Opti-MEM at room temperature for 15 min. Subsequently, the cells were incubated in medium for 24 h, and then harvested for assays.

Cell Proliferation Assay

A Cell Counting Kit-8 (CCK-8) was used to examine tumor cell proliferation according to the manufacturer's instructions. Transfected A549 cells were seeded onto 96-well culture plates at a density of 1×10^5 cells $\cdot 100 \mu\text{L}^{-1} \cdot \text{well}^{-1}$; then, 10 μL of the CCK-8 solution was added to each well and incubated for 2 h. An enzyme labeling instrument was used to read the optical density of the well.

Cell Migration Assay

Transfected A549 cells were trypsinized into a single-cell suspension, and then seeded onto a 24-well Transwell chamber (3428, Corning, NY, USA) at a density of 1×10^5 cells/well. After incubation for 24h at 37°C in a cell incubator, the transmembranes were fixed in 4% paraformaldehyde for 10 min, and then washed 3 times with PBS. After washing, a DAPI solution containing an anti-quenching agent was added to the bottom of the upper chamber for imaging using a fluorescence microscope.

Cell Apoptosis Assay

A549 cells were inoculated on the 6-well plate on average. Transfection of STIP1 shRNA was performed when the cells had reached approximately 70% confluence. After 24h, the cells were stained with Hoechst33258 (2 $\mu\text{g/mL}$) for 60 min at 37°C. Staining was observed and imaged under an inverted fluorescence microscope.

Apoptosis was also detected by flow cytometry. Transfected A549 cells were trypsinized with trypsin without EDTA into a single-cell suspension, and then washed twice with PBS. The cells were resuspended and mixed with 500 μL of 1 \times binding buffer, and then with AnnexinV-FITC and propidium iodide. After incubation at room temperature for 15 min in the dark, apoptosis was assessed by flow cytometry.

Cell Adhesion Assay

A549 cells were cultured in 96-well plates. Transfection of STIP1 shRNA was performed when the cells had reached approximately 70% confluence. After 24 h, the cells were stained with Giemsa for 30 min. After staining, the OD value was measured at 570 nm by enzyme label. The adhesion rate was calculated as $(\text{OD1}/\text{OD0}) \times 100\%$, where OD1 represents the treatment group and OD0 the control group.

Cell Movement and Migration Analysis

A549 cells were cultured in 6-well plates. Transfection of STIP1 shRNA was performed when the cells had reached approximately 70% confluence. After 24 h, the cells were scribed, and then washed and imaged. Image ProPlus software (IPP6.0) was used to analyze the distance between cells in each selected location and scratches, and calculate the actual cell migration rate. GraphPad Prism 5.0 (GraphPad Software, Inc., San Diego, CA, USA) was used for statistical analysis.

Tumor Formation in Nude Mice by Xenotransplantation of STIP1 shRNA-Expressing Cells

A549 cells (1×10^6) transfected with shRNA were hypodermic injected through groin into nude mice ($n = 6$ per group). All the mice were euthanized five weeks after injection. The lungs were then excised from the mice and fixed in 4% paraformaldehyde and liquid nitrogen. Lung tissues were sectioned and used for histological analysis.

Statistical Analysis

SPSS19.0 software was used for statistical analysis. Data were expressed as means \pm standard deviation (SD). A *t*-test was used for comparison between two groups, and one-way ANOVA was used for comparison between multiple groups. Counting data were expressed as number or rate. The chi-squared test was also used for statistical analysis. All tests were two-sided, and *p*-values < 0.05 were considered significant.

Results

STIP1 Is Highly Expressed in Lung Adenocarcinoma and Is Related to TNM Stage and Lymph Node Metastasis

To determine the expression of STIP1 in lung cancer, we employed immunohistochemistry to investigate the expression and localization of STIP1 in tissue obtained from 48 lung adenocarcinoma and 32 lung squamous cell carcinoma patients, and analyzed the relationship between the STIP1 expression and the clinicopathological features of the patients. STIP1 immunoreactivity was observed mainly in the cytoplasm, but was also detected in the nucleus (Figure 1). A significant difference in STIP1 expression was observed between lung cancer and paracancerous tissue; STIP1 expression was almost undetectable in 80 lung paracancerous tissue samples analyzed, but was variably expressed in 80 lung adenocarcinoma and lung squamous cell carcinoma tissue samples (Figure 1).

Further analysis indicated that the average immunohistochemical score for STIP1 expression was 3.86 ± 0.34 in 32 lung squamous cell carcinoma samples and 8.19 ± 0.41 in 48 lung adenocarcinoma samples. A significant difference was recorded in the average immunohistochemical score for STIP1 expression between lung squamous cell carcinoma and lung adenocarcinoma ($P < 0.05$, Table 1). In addition, STIP1 expression in lung cancer was associated with pathological classification, lymph node metastasis, and TNM stage ($P < 0.05$), but not sex, age, and smoking (Table 2).

Next, we employed RT-qPCR and Western blotting to assess STIP1 mRNA and protein expression levels in lung adenocarcinoma tumor tissue and corresponding paracancerous tissue. The results indicated that the level of STIP1 expression in lung adenocarcinoma tissue was higher than that in paracancerous tissue at both the mRNA and protein level (Figure 2A and B). To determine the most suitable cell line for our experiments, we first screened STIP1 expression

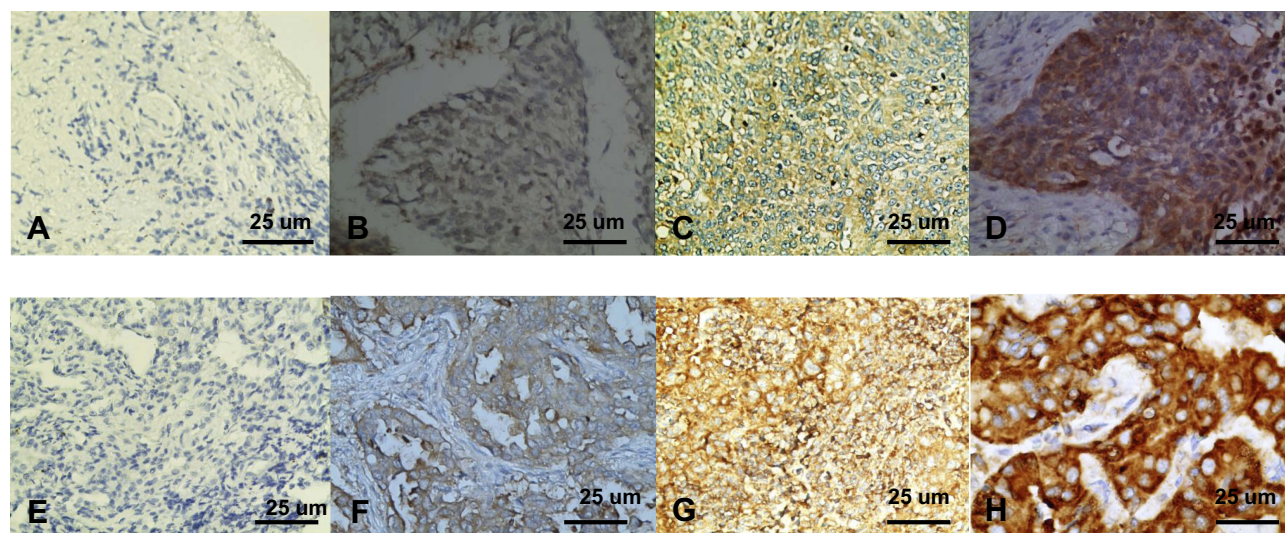


Figure 1 Immunohistochemical analysis of STIP1 expression in lung cancer and paracancerous tissue ($\times 400$). (A) STIP1 staining was almost undetectable in tissue adjacent to LSCC. (B) Weak STIP1 staining in LSCC tissue. (C) Moderate STIP1 staining in LSCC tissue. (D) Strong STIP1 staining in LSCC tissue. (E) STIP1 staining was almost undetectable in tissue adjacent to LAC. (F) Weak STIP1 staining in LAC tissue. (G) Moderate STIP1 staining in LAC tissue. (H) Strong STIP1 staining in LAC tissue. **Abbreviations:** LSCC, lung squamous cell carcinoma; LAC, lung adenocarcinoma.

in four lung adenocarcinoma cell lines. Because the expression level of STIP1 was highest in A549 cells (Figure 2C), this cell line was adopted for use in subsequent cytological experiments. We assessed expression levels in A549 and HBE cells. The results showed that STIP1 mRNA and protein expression levels were significantly higher in A549 cells than those in HBE cells ($P < 0.05$) (Figure 2D and E). These results demonstrated that STIP1 was strongly expressed in lung adenocarcinoma and may play an important role in its pathogenesis.

STIP1 Promoted Proliferation, Adhesion, Movement, and Migration, and Inhibited Apoptosis, in Lung Adenocarcinoma Cells

To study the role and mechanism responsible for the high expression of STIP1 in lung adenocarcinoma, we employed shRNA to assess the effect of downregulating STIP1 expression on lung adenocarcinoma cells. Four

groups of synthetic shRNAs were initially transfected into A549 cells to determine which shRNA was the most effective at reducing STIP1 expression. Western blotting results indicated that shRNA1 elicited the greatest reduction in STIP1 expression levels ($P < 0.05$, Figure 3A) and was selected for subsequent transfection experiments.

To assess the effect of STIP1 on lung adenocarcinoma cell proliferation, a CCK-8 assay was conducted. The results indicated that the relative CCK-8 value in the shRNA-transfected group was significantly lower than that in the control group ($P < 0.05$, Figure 3B). Next, Giemsa staining was used to investigate the effect of STIP1 on the cell adhesive ability of lung adenocarcinoma cells. The results showed that the relative value for cell adhesive ability in the shRNA-transfected group was markedly lower than that in the control group ($P < 0.05$, Figure 3C). Together, these results indicated that STIP1 enhanced the proliferative and adhesive capacity of lung adenocarcinoma cells.

A scratch test was carried out to analyze the effect of STIP1 on the migratory ability of lung adenocarcinoma cells. We found that the relative value for the migratory ability of lung adenocarcinoma cells transfected with STIP1 shRNA was distinctly lower than that of the non-transfected controls ($P < 0.05$, Figure 3D). In addition to the cell scratch test, the migratory capacity of lung adenocarcinoma cells was also evaluated by transwell migration assay. The results indicated that the migratory ability of lung adenocarcinoma cells transfected with STIP1 shRNA was considerably lower than that of nontransfected cells

Table 1 Comparison of Average Immunohistochemical Scores Between Lung Squamous Cell Carcinoma and Lung Adenocarcinoma (Score, Mean \pm Standard Deviation)

| Pathological Type | N | Score |
|-------------------|----|-----------------|
| LSCC | 32 | 3.86 \pm 0.34 |
| LAC | 48 | 8.19 \pm 0.41 |
| t-value | | 1.28 |
| P-value | | <0.05 |

Abbreviations: LAC, lung adenocarcinoma; LSCC, lung squamous cell carcinoma.

Table 2 Correlation Between STIP1 Expression and Clinicopathological Features in Lung Cancer

| Parameter | Group | N | Expression of STIP1 | | | | |
|--------------------|--------|----|---------------------|--------------|-----------|----------|---------|
| | | | Weak(%) | Moderate (%) | Strong(%) | χ^2 | P-Value |
| Age | <60 | 30 | 8(26.67) | 12(40) | 10(33.33) | 3.68 | >0.05 |
| | ≥60 | 50 | 17(34.0) | 14(28.0) | 19(38.0) | | |
| Gender | Male | 44 | 14(31.82) | 12(27.27) | 18(40.91) | -1.25 | >0.05 |
| | Female | 36 | 12(33.33) | 14(38.89) | 12(33.33) | | |
| Smoking | 0 | 32 | 11(34.37) | 10(31.25) | 11(34.38) | 1.23 | >0.05 |
| | 0.1–30 | 16 | 4(25.0) | 6(37.5) | 6(37.5) | | |
| | >30 | 32 | 9(28.13) | 11(34.38) | 12(37.50) | | |
| Histology | LAC | 48 | 6(12.5) | 11(22.92) | 31(64.58) | 3.32 | <0.05* |
| | LSCC | 32 | 14(43.75) | 12(37.5) | 6(18.75) | | |
| Lymphatic invasion | N0 | 38 | 14(36.84) | 16(42.1) | 8(21.05) | 1.59 | <0.05* |
| | N1 | 21 | 5(23.81) | 6(28.57) | 10(47.62) | | |
| | N2 | 15 | 1(6.67) | 1(6.67) | 13(86.66) | | |
| | N3 | 6 | 0(0) | 0(0) | 6(100.0) | | |
| TNM stage | I | 15 | 9(60.0) | 4(26.67) | 2(13.33) | 3.45 | <0.05* |
| | II | 31 | 10(32.26) | 13(41.94) | 8(25.8) | | |
| | III | 29 | 1(3.45) | 5(17.24) | 23(79.31) | | |
| | IV | 5 | 0(0) | 1(20.0) | 4(80.0) | | |

Note: *Indicates a significant difference at $P < 0.05$.

Abbreviations: LAC, lung adenocarcinoma; LSCC, lung squamous cell carcinoma; Smoking, pack years of smoking.

($P < 0.05$, Figure 3E). These results indicate that STIP1 is involved in lung adenocarcinoma cell migration.

Hoechst staining was employed to determine whether STIP1 was important for the viability of lung adenocarcinoma cells. We found that the number of apoptotic cells was significantly higher in the STIP1 shRNA-transfected group than in the nontransfected control group ($P < 0.05$, Figure 3F). In addition to Hoechst staining, we also tested the effect of STIP1 downregulation on the viability of lung adenocarcinoma cells by flow cytometry. The results showed that the proportion of apoptotic cells in the transfected group was significantly higher than that in the control, nontransfected group ($P < 0.05$, Figure 3G). The results imply that STIP1 inhibited the apoptosis of lung adenocarcinoma cells.

STIP1 May Be Involved in the JAK2/STAT3 Signaling Pathway and EMT

To explore whether STIP1 affects the JAK2/STAT3 signaling pathway, we analyzed the effect of STIP1 on JAK2 and STAT3 protein levels. No significant difference was recorded in JAK2 and STAT3 expression levels between the shRNA-transfected and control, nontransfected groups (Figure 4A). However, the levels of phosphorylated JAK2 (p-JAK2) and STAT3 (p-STAT3) in transfection group were

significantly lower in the STIP1 shRNA-transfected group than in the control, nontransfected group ($P < 0.05$, Figure 4A). These results imply that STIP1 may be involved in lung adenocarcinoma recurrence and metastasis through the activation of the JAK2/STAT3 signaling pathway.

We next tested the effect of STIP1 on E-cadherin and vimentin protein expression. The expression of E-cadherin in the STIP1 shRNA-transfected group was significantly higher than that in the nontransfected control group ($P < 0.05$, Figure 4B), whereas that of vimentin exhibited the opposite trend ($P < 0.05$, Figure 4B), suggesting that STIP1 may play a role in EMT in lung adenocarcinoma cells.

STIP1 May Be Involved in the JAK2/STAT3 Signaling Pathway and EMT of STIP1 shRNA-Induced Tumors in Nude Mice

To further confirm the role and mechanism of STIP1 in lung adenocarcinoma, we established a xenotransplantation model of lung adenocarcinoma in nude mice. Tumor volume in nude mice injected with STIP1 shRNA-transfected A549 cells was significantly lower than that of nude mice injected with nontransfected A549 cells ($P < 0.05$, Figure 5A and B), indicating that STIP1 shRNA markedly suppressed the

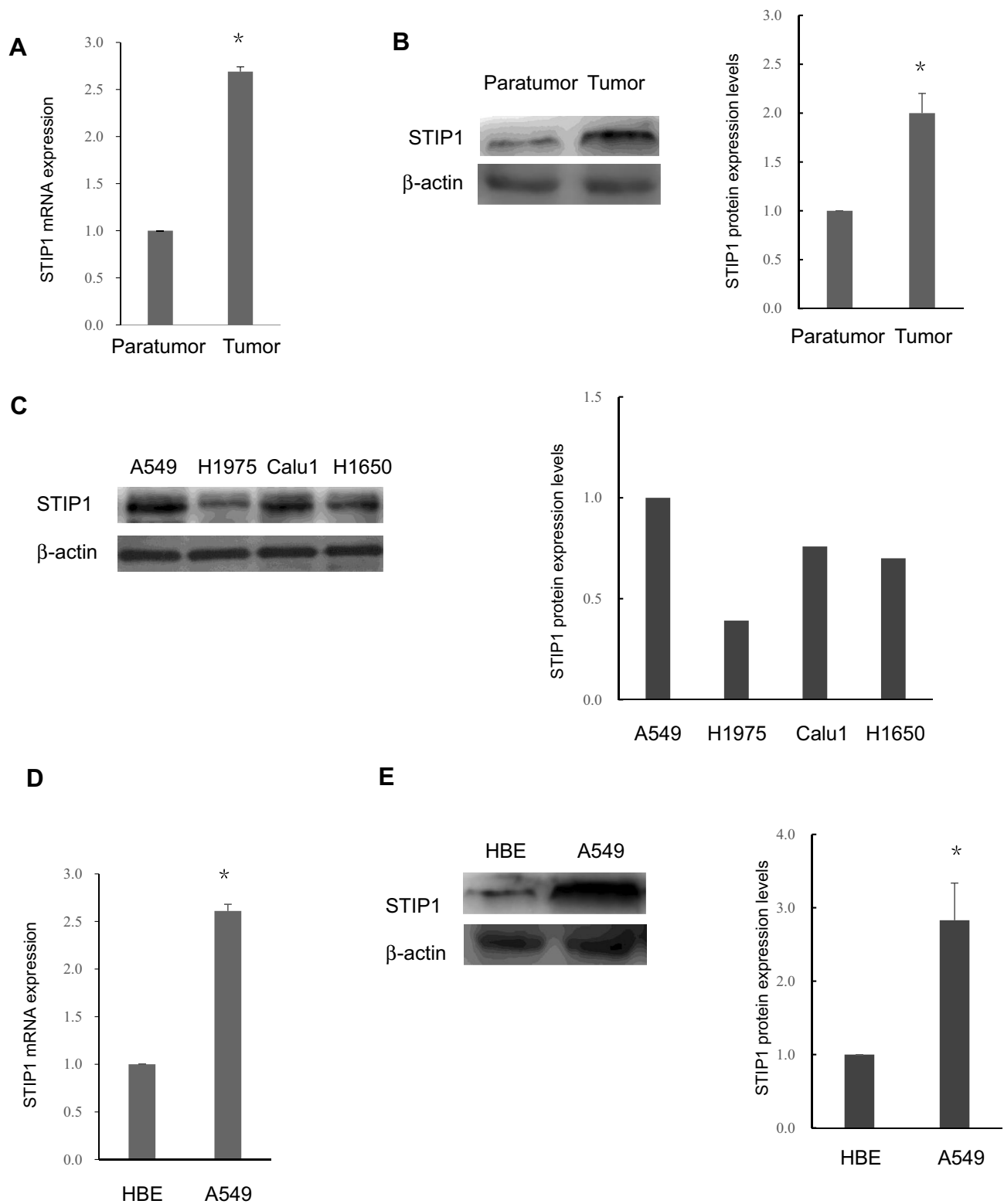


Figure 2 STIP1 was strongly expressed at both the mRNA and protein level in lung adenocarcinoma tissue and cells. **(A)** The *STIP1* mRNA expression level in lung adenocarcinoma tissue was significantly higher than that in adjacent tissue ($*P<0.05$). **(B)** The STIP1 protein expression level in lung adenocarcinoma tissue was markedly higher than that in adjacent tissue ($*P<0.05$). **(C)** The STIP1 expression level was relatively high in A549 cells. **(D)** The *STIP1* mRNA expression level in A549 cells was considerably higher than that in normal human bronchial epithelial (HBE) cells ($*P<0.05$). **(E)** The STIP1 protein expression level in A549 cells was markedly higher than that in HBE cells ($*P<0.05$).

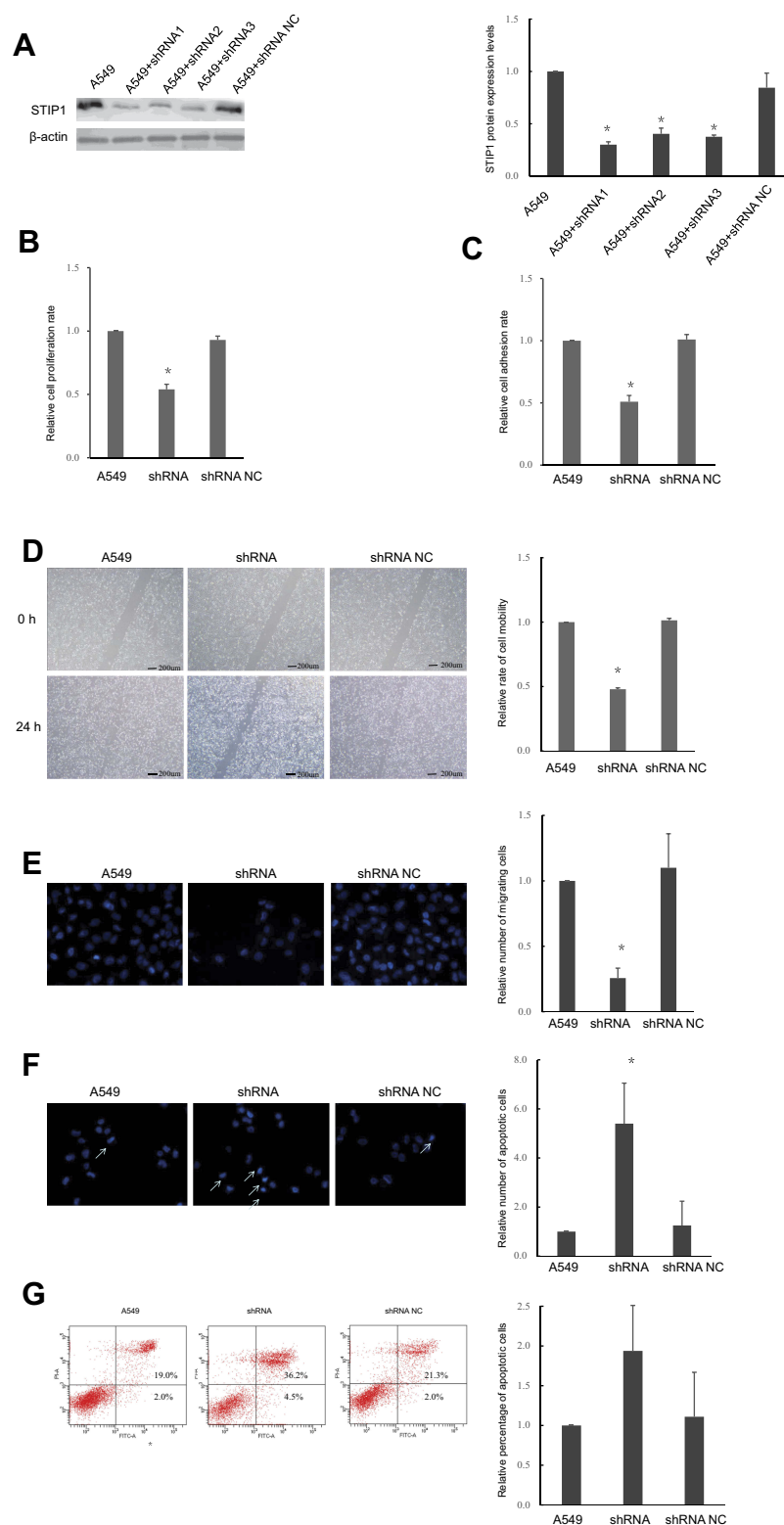


Figure 3 Transfection of STIP1 shRNA enhanced the proliferative, adhesive, and migratory ability, and suppressed the apoptosis, of A549 lung adenocarcinoma cells. **(A)** Compared with the control and other shRNAs, STIP1 shRNA1 was the most effective at reducing STIP1 expression (* $P < 0.05$). **(B)** Transfection of STIP1 shRNA led to a significant decrease in the proliferative ability of lung adenocarcinoma cells (* $P < 0.05$). **(C)** Transfection of STIP1 shRNA led to a significant reduction in the adhesive ability of lung adenocarcinoma cells (* $P < 0.05$). **(D)** Transfection of STIP1 shRNA led to a marked decline in mobility of lung adenocarcinoma cells (* $P < 0.05$). **(E)** Transfection of STIP1 shRNA led to a significant reduction in migratory ability of lung adenocarcinoma cells (* $P < 0.05$). **(F, G)** Transfection of STIP1 shRNA led to a significant increase in the apoptosis of lung adenocarcinoma cells (* $P < 0.05$).

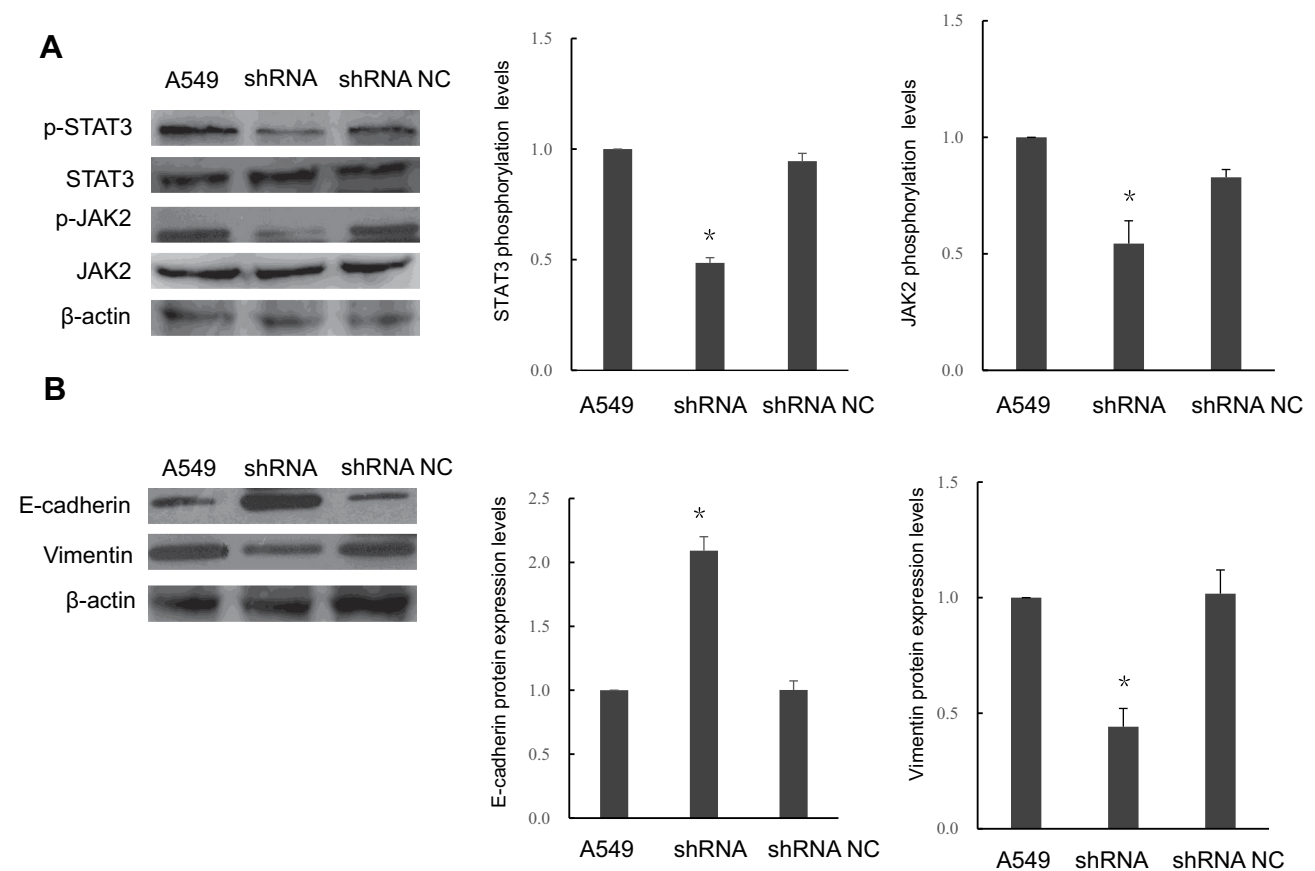


Figure 4 Transfection of STIP1 shRNA led to a reduction in the level of JAK2 and STAT3 phosphorylation and epithelial-to-mesenchymal transition. **(A)** STIP1 shRNA transfection resulted in reduced levels of p-JAK2 and p-STAT3 (* $P < 0.05$), but did not affect JAK2 or STAT3 protein levels. **(B)** Transfection of STIP1 shRNA led to upregulation of E-cadherin expression and suppression of vimentin expression (* $P < 0.05$).

growth of lung adenocarcinoma. To clarify the expression of STIP1 protein in the induced tumors, the protein level of STIP1 was examined by both immunohistochemistry and Western blot. The immunohistochemistry results showed that STIP1 protein expression in the nude mice injected with nontransfected A549 cells was high, while that of nude mice injected with STIP1-transfected A549 cells was low (Figure 5C). These results were further confirmed by Western blot ($P < 0.05$, Figure 5D). These in vivo results provided strong evidence that the expression level of STIP1 in lung adenocarcinoma was related to the formation of lung adenocarcinoma.

To further confirm the role of STIP1 in lung adenocarcinoma in vivo, we also investigated the effect of STIP1 on the JAK2/STAT3 signaling pathway and EMT in the nude mice. The levels of p-JAK2 and p-STAT3 in nude mice injected with STIP1 shRNA-transfected A549 cells were significantly lower than that in nude mice injected with A549 cells ($P < 0.05$, Figure 5E), suggesting that STIP1 downregulation reduced the levels of p-JAK2

and p-STAT3. Moreover, E-cadherin expression in the tumors of nude mice injected with STIP1 shRNA-transfected A549 cells was significantly higher ($P < 0.05$, Figure 5F) than that of nude mice injected with nontransfected A549 cells. However, vimentin expression levels exhibited the opposite trend ($P < 0.05$, Figure 5F). These results showed that downregulation of STIP1 induced E-cadherin protein expression and inhibited that of vimentin, suggesting that STIP1 downregulation inhibited EMT progression. Combined, the above observations imply that STIP1 may be involved in EMT processes through the activation of the JAK2/STAT3 signaling pathway, thereby accelerating lung adenocarcinoma growth and metastasis.

Discussion

STIP1 acts as a co-chaperone of the HSP70/HSP90 molecular complex. Recent studies have shown that STIP1 is highly expressed in thyroid papillary carcinoma, ovarian cancer, and liver cancer, as well as other tumors.^{15–20} Although STIP1 has been associated with tumor

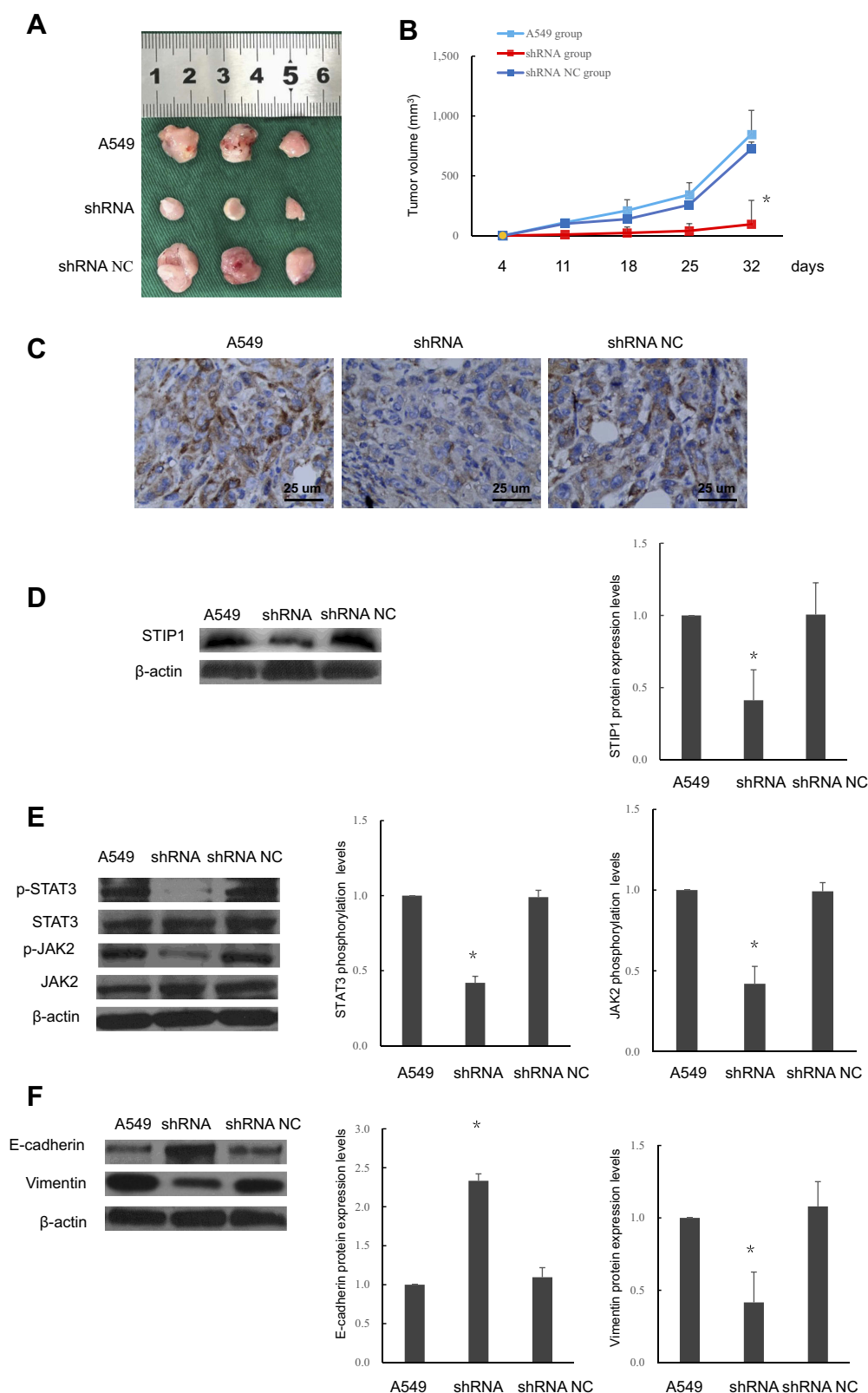


Figure 5 Effects of STIP1 on tumorigenesis in nude mice and associated mechanisms. **(A, B)** Tumor growth in nude mice injected with A549 lung adenocarcinoma cells transfected with STIP1 shRNA was reduced compared with that in nontransfected cells and those transfected with the negative control (* $P < 0.05$). **(C)** Immunohistochemistry indicated that transfection with STIP1 shRNA led to a reduction in STIP1 protein levels in mouse tumors ($\times 400$). **(D)** Western blot showing that STIP1 shRNA suppressed STIP1 protein levels in mouse tumors (* $P < 0.05$). **(E)** Transfection with STIP1 shRNA led to a reduction in the levels of phosphorylated JAK2 and STAT3 in STIP1 shRNA-induced tumors in nude mice (* $P < 0.05$). **(F)** Transfection with STIP1 shRNA led to the upregulation of E-cadherin expression and suppression of vimentin expression (* $P < 0.05$).

occurrence and development, no studies have described the expression patterns and roles of STIP1 in lung adenocarcinoma. In our study, we found that STIP1 is highly expressed in lung adenocarcinoma, indicating that STIP1 may play an important role in the occurrence and development of this cancer. To further explore the role of STIP1 in lung adenocarcinoma, we examined whether downregulating STIP1 expression affected the proliferative and migratory ability of lung adenocarcinoma cells. Our results suggest that STIP1 can enhance the proliferative, adhesive, and migratory ability, inhibit the apoptosis, and accelerate the growth, of lung adenocarcinoma. This is consistent with the results reported for STIP1 in melanoma.²²

STIP1 is involved in tumor proliferation and growth through several signaling pathways. STIP1 increases the metastatic potential, inhibits the apoptosis, and promotes the growth of hepatocellular carcinoma cells through the PI3K-Akt and β -catenin/TCF pathways.²³ In gastric cancer, STIP1 participates in the EMT process and increases the invasive and metastatic ability of gastric cancer cells by acting on its target genes, c-Myc and cyclinD1, through the Wnt/ β -catenin signaling pathway.²⁴ In melanoma, the elevated expression of STIP1 increases tumor metastasis by promoting cell proliferation and suppressing apoptosis through JAK2/STAT3 signaling.²² The results of our study indicate that STIP1 may induce proliferation and growth in lung adenocarcinoma by activating the JAK2/STAT3 signaling pathway and participating in EMT. Our in vivo experiments in mice further showed that STIP1 promotes tumor growth through the JAK2/STAT3 signaling pathway. In addition to the JAK2/STAT3 signaling pathway proposed in this study, other pathways may exist through which STIP1 induces the proliferation and growth of lung adenocarcinoma, such as the ERK, Wnt/ β -catenin, and PI3K/Akt signaling pathways. However, whether STIP1 also affects these signaling pathways requires further investigation.

In addition, the mechanism through which STIP1 acts on the JAK2/STAT3 signaling pathway also requires further investigation. STIP1, HSP70, and HSP90 are all highly expressed and interact in colon cancer tissue,²⁵ while HSP90 acts on Akt to promote cell growth and inhibit apoptosis.²⁶ STIP1 can also interact with gene promoters; for example, STIP1 can accelerate SMAD protein binding to the *ID3* promoter, thereby enhancing ovarian cancer cell proliferation and growth.²⁷ Combined, the results of this study suggest that STIP1 may interact with

HSP70/HSP90 or other proteins to activate the JAK2/STAT3 signaling pathway in lung adenocarcinoma. So it needs to be investigated that what's the protein of binding to STIP1 and whether it is related to the three TPR domains in STIP1. In the future, we will analyze in detail the structural basis among STIP1, HSP70/HSP90, and JAK2 to further reveal the STIP1 mechanisms of action in lung adenocarcinoma.

Conclusion

In this study, we aimed to identify a therapeutic target for early screening and treatment of lung adenocarcinoma. We have shown that STIP1 plays a role in the development of this cancer, and that this may occur through the JAK2/STAT3 signaling pathway. In the future, we will perform more detailed investigation to provide a firm scientific basis for the therapeutic application of STIP1 in lung adenocarcinoma.

Acknowledgments

This research was supported by the Precision Medicine Research of The National Key Research and Development Plan of China (2016YFC0905800), National Natural Science Foundation of China (81970031, 81770031, 81700028), and Natural Science Foundation of Jiangsu Province (BK20181497, BK20171501, BK20171080).

Disclosure

The authors report no conflicts of interest in this work.

References

1. Bray F, Ferlay J, Soerjomataram I, et al. Global cancer statistics 2018: GLOBOCAN estimates of incidence and mortality worldwide for 36 cancers in 185 countries. *CA Cancer J Clin*. 2018;68(6):394–424. doi:10.3322/caac.21492
2. Zheng R, Zeng H, Zhang S, et al. Cancer incidence and mortality in China, 2013. *Chin J Cancer*. 2017;36(1):66. doi:10.1016/j.canlet.2017.04.024
3. Choi JE, Bae JS, Kang MJ, et al. Expression of epithelial-mesenchymal transition and cancer stem cell markers in colorectal adenocarcinoma: clinicopathological significance. *Oncol Rep*. 2017;38(3):1695–1705. doi:10.3892/or.2017.5790
4. Niknami Z, Eslamifar A, Emamirazavi A, et al. The association of vimentin and fibronectin gene expression with epithelial-mesenchymal transition and tumor malignancy in colorectal carcinoma. *EXCLI J*. 2017;16:1009. doi:10.17179/excli2017-481
5. Wu L, Li J, Liu T, et al. Quercetin shows anti-tumor effect in hepatocellular carcinoma LM3 cells by abrogating JAK2/STAT3 signaling pathway. *Cancer Med*. 2019;8(10):4806–4820. doi:10.1002/cam4.2388
6. Lu Z, Lu C, Li C, et al. Dracorhodin perchlorate induces apoptosis and G2/M cell cycle arrest in human esophageal squamous cell carcinoma through inhibition of the JAK2/STAT3 and AKT/FOXO3a pathways. *Mol Med Rep*. 2019;20(3):2091–2100. doi:10.3892/mmr.2019.10474

7. Mohr A, Chatain N, Domoszlai T, et al. Dynamics and non-canonical aspects of JAK/STAT signaling. *Eur J Cell Biol*. 2012;91(6-7):524–532. doi:10.1016/j.ejcb.2011.09.005
8. Kim BI, Kim JH, Sim DY, et al. Inhibition of JAK2/STAT3 and activation of caspase 9/3 are involved in KYS05090S induced apoptosis in ovarian cancer cells. *Int J Oncol*. 2019;55:203–210. doi:10.3892/ijo.2019.4795
9. Yue P, Zhang X, Paladino D, et al. Hyperactive EGF receptor Jaks and Star3 signaling promote enhanced colony-forming ability, motility and migration of cisplatin-resistant ovarian cancer cells. *Oncogene*. 2012;31(18):2309–2322. doi:10.1038/onc.2011.409
10. Chen Z, Du Y, Liu X, et al. EZH2 inhibition suppresses bladder cancer cell growth and metastasis via the JAK2/STAT3 signaling pathway. *Oncol Lett*. 2019;18(1):907–915. doi:10.3892/ol.2019.10359
11. Nicolet CM, Craig EA. Isolation and characterization of STIP1, a stress-inducible gene from *Saccharomyces cerevisiae*. *Mol Cell Biol*. 1989;9:3638–3646. doi:10.1128/mcb.9.9.3638
12. Du C, Han YL, Hou CC, et al. Expression pattern of heat shock protein 90AB (HSP90AB) and stress-inducible protein 1 (Stip1) during spermatogenesis of mudskipper *Boleophthalmus pectinirostris*. *Comp Biochem Physiol B Biochem Mol Biol*. 2019;231:42–51. doi:10.1016/j.cbpb.2019.01.016
13. Chaudhary R, Baranwal VK, Kumar R, et al. Genome-wide identification and expression analysis of Hsp70, Hsp90, and Hsp100 heat shock protein genes in barley under stress conditions and reproductive development. *Funct Integr Genomics*. 2019;19(6):1007–1022. doi:10.1007/s10142-019-00695-y
14. Kituyi SN, Edkins AL. Hop/STIP1 depletion alters nuclear structure via depletion of nuclear structural protein emerlin. *Biochem Biophys Res Commun*. 2018;507(1–4):503–509. doi:10.1016/j.bbrc.2018.11.073
15. Sun W, Xing B, Sun Y, et al. Proteome analysis of hepatocellular carcinoma by two-dimensional difference gel electrophoresis novel protein markers in hepatocellular carcinoma tissues. *Mol Cell Proteomics*. 2007;6(10):1798–1808. doi:10.1074/mcp.M600449-MCP200
16. Carvalho da Fonseca AC, Wang H, Fan H, et al. Increased expression of stress inducible protein 1 in glioma-associated microglia/macrophages. *J Neuroimmunol*. 2014;274(1–2):71–77. doi:10.1016/j.jneuroim.2014.06.021
17. Walsh N, O'Donovan N, Kennedy S, et al. Identification of pancreatic cancer invasion-related proteins by proteomic analysis. *Proteome Sci*. 2009;7:3. doi:10.1186/1477-5956-7-3
18. Boysen M, Kityk R, Mayer MP. Hsp70- and Hsp90-mediated regulation of the conformation of p53 DNA binding domain and p53 cancer variants. *Mol Cell*. 2019;74(4):831–843. doi:10.1016/j.molcel.2019.03.032
19. Van Simaey D, Turek D, Champanhac C, et al. Identification of cell membrane protein stress-induced phosphoprotein 1 as a potential ovarian cancer biomarker using aptamers selected by cell systematic evolution of ligands by exponential enrichment. *Anal Chem*. 2014;86(9):4521–4527. doi:10.1021/ac500466x
20. Cho H, Kim S, Shin HY, et al. Expression of stress-induced phosphoprotein1 (STIP1) is associated with tumor progression and poor prognosis in epithelial ovarian cancer. *Genes Chromosomes Cancer*. 2014;53(4):277–288. doi:10.1002/gcc.22136
21. Wang L, Wei D, Huang S, et al. Transcription factor Sp1 expression is a significant predictor of survival in human gastric cancer. *Clin Cancer Res*. 2003;9(17):6371–6380.
22. Sun X, Cao N, Mu L, et al. Stress induced phosphoprotein 1 promotes tumor growth and metastasis of melanoma via modulating JAK2/STAT3 pathway. *Biomed Pharmacother*. 2019;116:108962. doi:10.1016/j.biopha.2019.108962
23. Chen L, Xu L, Su T, et al. Autocrine STIP1 signaling promotes tumor growth and is associated with disease outcome in hepatocellular carcinoma. *Biochem Biophys Res Commun*. 2017;493(1):365–372. doi:10.1016/j.bbrc.2017.09.016
24. Huang L, Zhai E, Cai S, et al. Stress-inducible protein-1 promotes metastasis of gastric cancer via Wnt/β-catenin signaling pathway. *J Exp Clin Cancer Res*. 2018;37(1):6. doi:10.1186/s13046-018-0676-8
25. Dahiya V, Agam G, Lawatscheck J, et al. Coordinated conformational processing of the tumor suppressor protein p53 by the Hsp70 and Hsp90 chaperone machineries. *Mol Cell*. 2019;74(4):816–830. doi:10.1016/j.molcel.2019.03.026
26. Lu R, Zhao G, Yang Y, et al. Inhibition of CD133 overcomes cisplatin resistance through inhibiting PI3K/AKT/mTOR signaling pathway and autophagy in CD133-positive gastric cancer cells. *Technol Cancer Res Treat*. 2019;18:1533033819864311. doi:10.1177/1533033819864311
27. Tsai C-L, Tsai C-N, Lin C-Y, et al. Secreted stress-induced phosphoprotein 1 activates the ALK2-SMAD signaling pathways and promotes cell proliferation of ovarian cancer cells. *Cell Rep*. 2012;2(2):283–293. doi:10.1016/j.celrep.2012.07.002

Cancer Management and Research

Publish your work in this journal

Cancer Management and Research is an international, peer-reviewed open access journal focusing on cancer research and the optimal use of preventative and integrated treatment interventions to achieve improved outcomes, enhanced survival and quality of life for the cancer patient.

Submit your manuscript here: <https://www.dovepress.com/cancer-management-and-research-journal>

Dovepress

The manuscript management system is completely online and includes a very quick and fair peer-review system, which is all easy to use. Visit <http://www.dovepress.com/testimonials.php> to read real quotes from published authors.